The final version of record is available at http://dx.doi.org/10.1109/TCOMM.2017.2657756

High SNR Error Analysis for Bidirectional Relaying with Physical Layer Network Coding

Karthik Ravindran, Andrew Thangaraj and Srikrishna Bhashyam
Department of Electrical Engineering
Indian Institute of Technology Madras, Chennai, India
Email: karthik.ravindran,andrew,skrishna@ee.iitm.ac.in

***Abstract*—We consider a large class of bidirectional relaying scenarios with physical layer network coding, and analytically characterize the relay's error performance in decoding the network-coded combination at high signal-to-noise ratio (SNR). Our analysis applies to scenarios with (1) binary or higher order real/complex modulation, (2) real or complex channel coefficients, and (3) linear or non-linear network maps for network coding at the relay. We consider block fading and allow the relay to choose from a set of network maps based on the channel coefficients of the source to relay links in every block. We derive expressions for pairwise error probability and approximate expected overall error probability. We also derive lower bounds for these error probabilities. We validate these expressions using simulations and show that our approximations are tight in the high SNR regime.**

I. INTRODUCTION

The bidirectional relaying setting is shown in Fig. 1. Nodes A and C wish to exchange messages. The relay node B facilitates this exchange of information. We assume that we do not have a direct link between the two communication nodes A and C. All the nodes are half-duplex with single antenna, and average power limited with receiver Additive White Gaussian Noise (AWGN) of variance σ_N^2. Channels AB (also, BA) and CB (also, BC) have coefficients which are denoted h_1 and h_2, respectively. The pair (h_1, h_2) is referred to as the channel fading state.

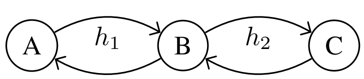

Fig. 1: Bidirectional relaying problem.

Bidirectional relaying was initially proposed in [1] [2] [3] and summarized in the surveys [4] [5]. Schemes based on lattice coding have been shown to achieve rates within a small gap of the capacity region [6], [7]. Practical codes based on finite alphabet constellations have been proposed in [8]–[14]. Most of the initial work in physical layer network coding for bidirectional relaying used binary modulation schemes and XOR decoding at the relay [8]. However, higher-order modulation schemes are required to achieve higher spectral efficiency. Bidirectional relaying with higher-order constellations were considered in [9]–[14]. Network coding maps for uncoded transmission were studied in [11]–[13]. Field-based network maps were used in [9], [10]. In [14], ring-based designs using Low-Density Parity-Check (LDPC) codes were proposed for standard M-PAM and M^2-QAM constellations. Both linear and non-linear network maps were used in [14]. Simulations were used to show the effectiveness of ring-based schemes over field-based schemes in [14].

The main goal of this work is to analytically compare different physical layer network coding strategies in terms of error performance at the relay. Specifically, we consider M-PAM or M^2-QAM constellations at transmit nodes A, C, and assume block fading with the channel coefficients h_1, h_2 following a real Gaussian distribution for M-PAM constellation and complex Gaussian distribution for M^2-QAM constellation. Depending on (h_1, h_2), the relay has a choice to decode one of many possible network maps (linear or non-linear). Under these assumptions, we derive the following in the limit $SNR \to \infty$:

1) Expected pairwise probability of error in decoding the network-coded combination.
2) Lower bound for the expected pairwise probability of error.
3) Approximate expected overall probability of error in decoding the network-coded combination.
4) Lower bound for the expected overall probability of error.

The computation of asymptotic expected error probabilities is done through the computation of the probability density function (PDF) of the *minimum cluster distance* in the relay's received constellation at 0 [15]. The minimum cluster distance is a function of the network map and channel coefficients h_1, h_2, and can become zero at some specific ratios of channel coefficients. We characterize the regions of (h_1, h_2) at which minimum cluster distance becomes zero, and use it to derive an analytical expression for the PDF at 0.

Error performance in bidirectional relaying has been studied before in [1], [16]–[20]. All of these works study specific strategies and are restricted in the modulation alphabet or network coding map, which are typically binary. Other related works from the compute-and-forward literature includes [21], [22], [23], [24], [16]. In [22] the authors use multilevel codes with XOR based network map, and also derive an upper bound on the decoding error probability. In [24], integer-linear network maps are considered, and bounds on decoding error probability are derived. In [16], the authors study the optimal methods of selecting coefficients of a linear network map, and also derive an upper bound for the probability of error. In most

This is the author's version of an article that has been published in this journal. Changes were made to this version by the publisher prior to publication.
The final version of record is available at http://dx.doi.org/10.1109/TCOMM.2017.2657756

of the above, linear network maps were considered.

In comparison with the earlier works relating to error performance characterization in bidirectional relaying, our work differs in the following ways:

1) The method of analysis using the PDF of minimum cluster distance at zero is new in the context of bidirectional relaying.
2) Our analysis applies to both linear and non-linear network maps for decoding at the relay, and higher-order M-PAM and M^2-QAM transmit constellations.
3) In our earlier work [14], we studied nonlinear network maps that maximized minimum cluster distance at the relay. The analysis in this work applies to [14] and justifies the use of minimum cluster distance as a metric.

II. Definitions and Notation

We consider bidirectional relaying with two phases - Multiple Access and Broadcast. In the multiple access phase, node A transmits $x_1 \in \mathcal{A}$, and node C transmits $x_2 \in \mathcal{A}$, where $\mathcal{A}$ is the constellation used at nodes A and C. The received value at the relay is given as

$$y_B = h_1 x_1 + h_2 x_2 + z_B,$$

where (h_1, h_2) are channel coefficients and z_B denotes additive Gaussian noise. We will assume Gaussian block fading, and that (h_1, h_2) are known to all nodes. The distribution of (h_1, h_2) will be assumed to be *iid* real Gaussian if $\mathcal{A}$ is real, and complex Gaussian if $\mathcal{A}$ is complex.

At the relay B, the received symbol $h_1 x_1 + h_2 x_2$ belongs to the constellation

$$\mathcal{M}_B = \{s(u, v) = h_1 u + h_2 v : u, v \in \mathcal{A}\}, \tag{1}$$

where $s : \mathcal{A}^2 \to \mathcal{M}_B$ is a many-to-one map, in general. That is, based on the values of h_1, h_2 and the constellation $\mathcal{A}$, some of the transmit symbol pairs in $\mathcal{A}^2$ may map to the same point in $\mathcal{M}_B$. We define a network map $f : \mathcal{A}^2 \to \mathcal{A}_{BC}$, where $\mathcal{A}_{BC}$ is the constellation used by the relay in the broadcast phase. We consider the scenario where the network map f is chosen in a specific manner, to be described later, based on h_1, h_2. For any given transmit symbol pair $(x_1, x_2) \in \mathcal{A}^2$ from nodes A and C, the relay attempts to decode $x_B = f(x_1, x_2) \in \mathcal{A}_{BC}$. Let the relay's decoded symbol be denoted $\hat{x}_B \in \mathcal{A}_{BC}$.

The symbol $\hat{x}_B \in \mathcal{A}_{BC}$ is broadcast by the relay B in the broadcast phase. The received values at the end nodes A and C are given as

$$y_A = h_1 \hat{x}_B + z_A,$$
$$y_C = h_2 \hat{x}_B + z_C,$$

where z_A and z_C denote additive Gaussian noise. Using the received value y_A, node A decodes $x_2 \in \mathcal{A}$ using the knowledge of its own transmitted symbol $x_1 \in \mathcal{A}$ and the map f. Node C decodes x_1 in a similar fashion using y_C.

A. Singular fading states and choice of network map

For a given constellation $\mathcal{A}$, a pair of non-zero channel coefficients (h_1, h_2) is said to be singular if there exist distinct pairs $(x_1, x_2), (x_1', x_2') \in \mathcal{A}^2$ such that $h_1 x_1 + h_2 x_2 = h_1 x_1' + h_2 x_2'$. For singular channel coefficients (h_1, h_2), the ratio $\frac{h_2}{h_1}$ is referred to as a singular fading state of $\mathcal{A}$ [13]. Clearly, the set of singular fading states is finite in number, and are given as the set of all distinct ratios of differences of constellation points. Let the set of singular fading states of $\mathcal{A}$ be denoted $\mathcal{S} = \{\alpha_1, \alpha_2, \ldots, \alpha_L\}$, where L is the number of singular fading states.

We consider the scenario where the choice of network map f is done as follows. We partition the (h_1, h_2)-space into $L+2$ non-overlapping (except at $(0, 0)$) regions $\Lambda_1, \Lambda_2, \ldots, \Lambda_{L+2}$ such that

1) the i-th singular fading states are contained in Λ_i, i.e., $\{(h_1, h_2) : \frac{h_2}{h_1} = \alpha_i\} \subset \Lambda_i$, $i = 1, 2, \ldots, L$,
2) the axis $h_1 = 0$ is contained in Λ_{L+1}, i.e., $\{(h_1, h_2) : h_1 = 0\} \subset \Lambda_{L+1}$,
3) the axis $h_2 = 0$ is contained in Λ_{L+2}, i.e., $\{(h_1, h_2) : h_2 = 0\} \subset \Lambda_{L+2}$.

Each region $\Lambda_i, i \in \{1, 2, \cdots L+2\}$ is associated to a network map f_i. If the channel coefficients $(h_1, h_2) \in \Lambda_i$, the relay sets $f = f_i$. No other constraint is placed on the regions Λ_i and the network maps f_i. Note that the f_i need not be unique, and two regions $\Lambda_i, \Lambda_j, i \neq j$ may be assigned the same map.

This scenario is generic and covers the strategies considered in [13], [14], [25]. As an example, we choose a 4-PAM transmit constellation with singular fading states $\mathcal{S} = \{\pm 1, \pm 2, \pm 3, \pm\frac{1}{3}, \pm\frac{2}{3}, \pm\frac{1}{2}, \pm\frac{3}{2}\}$ and illustrate in Figure 2, the partitioning of (h_1, h_2)-space into the regions $\Lambda_1, \Lambda_2, \cdots \Lambda_{16}$ (labeled $1, 2, \cdots 16$, respectively). Here, the adjacent regions are differentiated with different shades of gray, and the dashed lines correspond to $h_2 = \alpha_i h_1$.

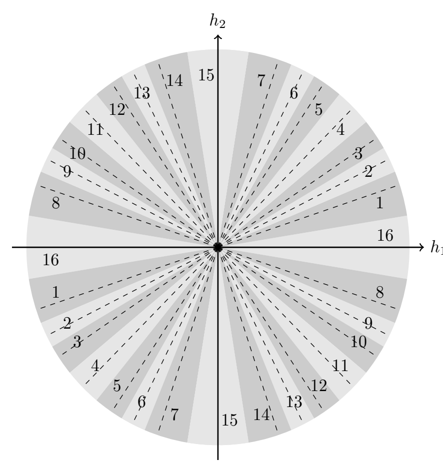

Fig. 2: Partitioning of (h_1, h_2)-space into different regions.

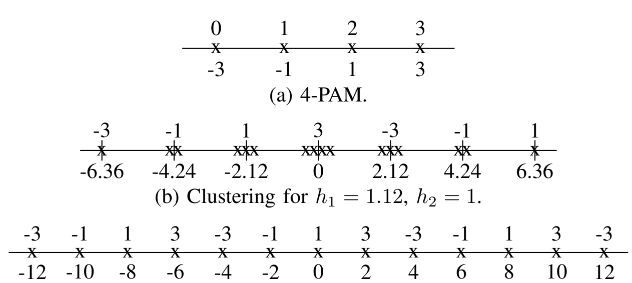

(a) 4-PAM.

(b) Clustering for $h_1 = 1.12$, $h_2 = 1$.

(c) Clustering for $h_1 = 3$, $h_2 = 1$

Fig. 3: Relay constellation and clustering for 4-PAM.

This is the author's version of an article that has been published in this journal. Changes were made to this version by the publisher prior to publication.
The final version of record is available at http://dx.doi.org/10.1109/TCOMM.2017.2657756

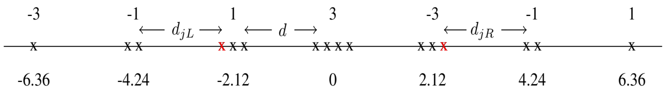

Fig. 4: Illustration of minimum cluster distance, left minimum cluster distance and right minimum cluster distance.

B. Minimum cluster distance and non-resolvable states

For $r \in \mathcal{A}_{BC}$, the set of pairs $f^{-1}(r) \triangleq \{(x_1, x_2) \in \mathcal{A}^2 : f(x_1, x_2) = r\}$ is referred to as a cluster mapped to r with respect to the network map f. One possible clustering is illustrated in Figure 3 for some channel coefficients, with $\mathcal{A}$ and $\mathcal{A}_{BC}$ set as 4-PAM. Here, the values in $\mathcal{M}_B$ are shown below the axis, while the cluster-mapped values $f(\cdot)$ of the symbol pairs corresponding to points in $\mathcal{M}_B$ are shown on top.

Since we are interested in characterizing the error performance in decoding the clusters at the relay, we define some distance metrics relating to distances between points in $\mathcal{M}_B$ corresponding to transmit pairs from different clusters.

The *minimum cluster distance* of the network map f at channel coefficients (h_1, h_2) is defined as the least distance between points (could be identical points) in $\mathcal{M}_B$ corresponding to transmit pairs from different clusters. That is,

$$d(f, h_1, h_2) \triangleq \min_{\substack{(x_1,x_2),(x_1',x_2') \in \mathcal{A}^2 \\ f(x_1,x_2) \neq f(x_1',x_2')}} |h_1(x_1 - x_1') + h_2(x_2 - x_2')|. \quad (2)$$

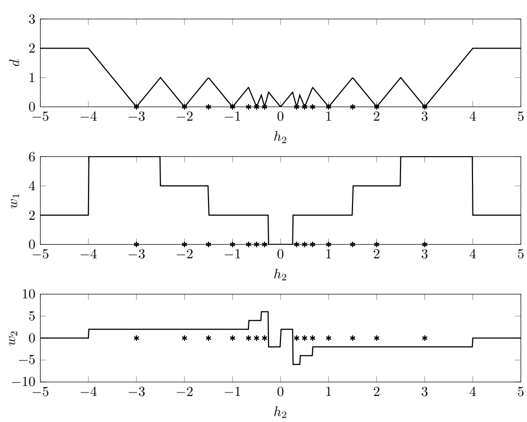

Fig. 5: Plots of $d = |w_1(h_1, h_2)h_1 + w_2(h_1, h_2)h_2|$, w_1 and w_2 versus h_2 with $\mathcal{A}$ being 4-PAM and $h_1 = 1$.

To reduce clutter, we will denote $d(f, h_1, h_2)$ as simply d some times. Minimum cluster distance in $\mathcal{M}_B$ with $\mathcal{A}$ set as 4-PAM and channel coefficients $h_1 = 1.12, h_2 = 1$ is illustrated in Figure 4. In this case, $d = 1.52$ corresponds to the distance between the points $r_1 = -1.88$ and $r_2 = -0.36$ in $\mathcal{M}_B$ corresponding to the transmit pairs $(1, -3)$ and $(-3, 3)$, respectively. We note that there are also other pairs of points in $\mathcal{M}_B$ whose distance between is $d = 1.52$.

From (2) we note that the minimum cluster distance is of the form $d = |w_1(h_1, h_2)h_1 + w_2(h_1, h_2)h_2|$, where the coefficients w_1 and w_2 depend on h_1, h_2. Additionally, we impose the constraint $w_1 \geq 0$ so that the relative sign between w_1 and w_2 is taken care by the sign of w_2. For illustration, in Figure 5, we plot d, w_1 and w_2 versus h_2, with $\mathcal{A} = \{-3, -1, 1, 3\}$ and $h_1 = 1$. Values of h_2 corresponding to the singular fading states of $\mathcal{A}$ are marked with $*$. The network map for a given h_2 is chosen based on the method described earlier, with each map f_i being a linear map over the field $\mathbb{F}_4$. From the plot of d we note that, at certain values of h_2 corresponding to some of the singular fading states, d is zero. Also, for regions around these singular fading states, w_1 and w_2 assume a constant value.

In general, for a given set of network maps, d can be zero at some singular fading states. If the transmitted pair $(x_1, x_2) \in \mathcal{A}^2$ is from a cluster whose distance from some other cluster is zero, a decoding error is likely to occur. A singular fading state $\alpha_i \in \mathcal{S}$ is said to be *non-resolvable* under the set of network maps $\{f_1, f_2, \ldots, f_{L+2}\}$ if the minimum cluster distance $d(f_i, 1, \alpha_i) = 0$. From the plot of d in Figure 5 we note that, in this case, the set of non-resolvable singular fading states is $\{\pm 1, \pm 2, \pm 3, \pm\frac{1}{3}, \pm\frac{1}{2}\}$. Let

$$\mathrm{NRI} = \{i : \alpha_i \text{ is non-resolvable}\} \quad (3)$$

be the set of indices of all non-resolvable singular fading states. This is useful for computing the pairwise error probability (to be defined later in this section) in decoding the clusters at the relay in the limit SNR tends to infinity.

Let us index the elements of $\mathcal{A}^2$ using $j = 1, 2, \cdots |\mathcal{A}|^2$. Let us consider the pair $(x_{1j}, x_{2j}) \in \mathcal{A}^2$. Next, we define the left and right minimum cluster distances with reference to the transmit pair (x_{1j}, x_{2j}). These are useful in computing the overall error probability in decoding at the relay, given that the transmitted pair is (x_{1j}, x_{2j}). The *left minimum cluster distance* of the network map f with reference to (x_{1j}, x_{2j}) at real channel coefficients (h_1, h_2), $\frac{h_2}{h_1} \notin \mathcal{S}$ is defined as the least difference between $h_1x_{1j} + h_2x_{2j} \in \mathcal{M}_B$ and points $\{h_1u + h_2v : (u, v) \in \mathcal{A}^2\}$ such that (i) $h_1u + h_2v$ is to the left of $h_1x_{1j} + h_2x_{2j}$, and (ii) (u, v) and (x_{1j}, x_{2j}) are from different clusters. That is,

$$d_{jL}(f, h_1, h_2) \triangleq \min_{\substack{(u,v) \in \mathcal{A}^2 \\ s(u,v) < s(x_{1j},x_{2j}) \\ f(x_{1j},x_{2j}) \neq f(u,v)}} |h_1(u - x_{1j}) + h_2(v - x_{2j})|.$$

If there exists no such $h_1u + h_2v \in \mathcal{M}_B$ satisfying the constraints mentioned above, we define $d_{jL}(f, h_1, h_2) = \infty$. We note that d_{jL} can be discontinuous at singular channel coefficients (h_1, h_2), $\frac{h_2}{h_1} \in \mathcal{S}$, and is therefore not defined at these values. As an example, the left minimum cluster distance in $\mathcal{M}_B$ with reference to the transmit pair $(-3, 1)$ is shown in Figure 4. In this case, $d_{jL} = 1.76$ corresponds to the distance between the points $r_1 = -2.36$ (marked in Red) and $r_2 = -4.12$ in $\mathcal{M}_B$ corresponding to the transmit pairs $(-3, 1)$ and $(-1, -3)$, respectively.

A singular fading state $\alpha_i \in \mathcal{S}$ is said to be *left-non-resolvable* with reference to $(x_{1j}, x_{2j}) \in \mathcal{A}^2$ under the set of network maps $\{f_1, f_2, \ldots, f_{L+2}\}$ if for every h_1, $\lim_{h_2 \to (\alpha_i h_1)^+} d_{jL}(f_i, h_1, h_2) = 0$ or $\lim_{h_2 \to (\alpha_i h_1)^-} d_{jL}(f_i, h_1, h_2) = 0$. Let

$$\mathrm{NRIL}(j) = \{i : \alpha_i \text{ is left-non-resolvable with reference to } (x_{1j}, x_{2j})\}$$

be the set of indices of all left-non-resolvable singular fading states with reference to $(x_{1j}, x_{2j}) \in \mathcal{A}^2$.

The *right minimum cluster distance* of the network map f with reference to (x_{1j}, x_{2j}) at real channel coefficients (h_1, h_2), $\frac{h_2}{h_1} \notin \mathcal{S}$ is defined as

$$d_{jR}(f, h_1, h_2) \triangleq \min_{\substack{(u,v)\in\mathcal{A}^2 \\ s(u,v)>s(x_{1j},x_{2j}) \\ f(x_{1j},x_{2j})\neq f(u,v)}} |h_1(u-x_{1j})+h_2(v-x_{2j})|.$$

This is similar to the left minimum cluster distance, except that we consider points in $\mathcal{M}_B$ to the right of $h_1x_{1j} + h_2x_{2j}$ to compute the minimum distance. In Figure 4, the right minimum cluster distance in $\mathcal{M}_B$ with reference to the transmit pair $(3, -1)$ is shown. A singular fading state $\alpha_i \in \mathcal{S}$ is said to be *right-non-resolvable* with reference to $(x_{1j}, x_{2j}) \in \mathcal{A}^2$ under the set of network maps $\{f_1, f_2, \ldots, f_{L+2}\}$ if for every h_1, $\lim_{h_2\to(\alpha_i h_1)^+} d_{jR}(f_i, h_1, h_2) = 0$ or $\lim_{h_2\to(\alpha_i h_1)^-} d_{jR}(f_i, h_1, h_2) = 0$. Let

$$\text{NRIR}(j) = \{i : \alpha_i \text{ is right-non-resolvable with reference to } (x_{1j}, x_{2j})\}$$

be the set of indices of all right-non-resolvable singular fading states with reference to (x_{1j}, x_{2j}). The sets of indices NRIL and NRIR are useful for computing the overall error probability in decoding at the relay in the limit SNR tends to infinity.

In Figure 6, we plot d_{jL} and d_{jR} with reference to $(x_{1j}, x_{2j}) = (-3, -1)$ versus h_2 with $\mathcal{A}$ being 4-PAM and $h_1 = 1$. We select the network map for a given h_2 from a set of linear maps over $\mathbb{F}_4$. From the plot we note that d_{jL} and d_{jR} can be discontinuous at certain values of h_2, which includes values of h_2 corresponding to some of the singular fading states of 4-PAM. Also, we note that, the set of left and right non-resolvable singular fading states with reference to $(x_{1j}, x_{2j}) = (-3, -1)$ is $\{-2, -1, 1, 3\}$.

For complex channel coefficients h_1, h_2, minimum cluster distance $d = |d'_R + id'_I|$, where d'_R and d'_I are the real and imaginary components of the difference $h_1(u_1-v_1)+h_2(u_2-v_2)$. Here, the transmit symbol pairs

$$(u_1, v_1),(u_2, v_2) = \arg \min_{\substack{(x_1,x_2),(x'_1,x'_2)\in\mathcal{A}^2 \\ f(x_1,x_2)\neq f(x'_1,x'_2)}} |h_1(x_1 - x'_1) + h_2(x_2 - x'_2)|$$

may not be unique for a given value of h_1, h_2, and network map f. We define the *minimum cluster distance vector* of the network map f at complex channel coefficients (h_1, h_2) as

$$D \triangleq [|d'_R| \quad |d'_I|].$$

C. Pairwise probability of errror

For given channel coefficients $(h_1, h_2) \in \Lambda_i$, we define the *pairwise probability of error* in decoding the clusters at the relay as

$$P_e(\Lambda_i) \triangleq Q\left(\frac{d(f_i, h_1, h_2)}{2\sigma_N}\right),$$

where σ_N^2 is the noise variance per dimension. We note that, in general, pairwise probability of error can be defined between any pair of clusters. In our case, we restrict ourselves to the clusters corresponding to the minimum cluster distance. We shall denote $P_e(\Lambda_i)$ as simply P_e. Later, we compute the expected pairwise probability of error ($E[P_e]$) when the channels are fading.

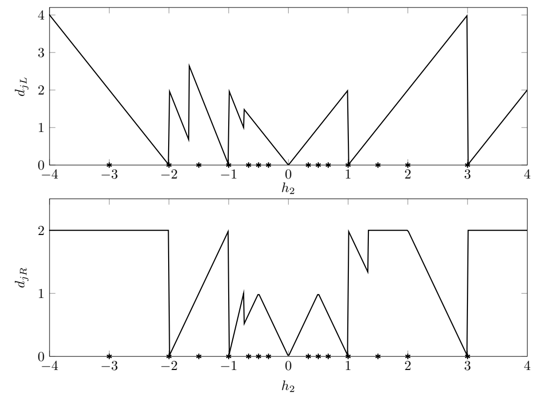

Fig. 6: Plots of d_{jL} and d_{jR} versus h_2 with $(x_{1j}, x_{2j}) = (-3, -1)$, $\mathcal{A}$ being 4-PAM and $h_1 = 1$.

III. M-PAM

In this section we consider the case of $\mathcal{A}$ being real M-PAM, and channel coefficients (h_1, h_2) being *iid* $\mathcal{N}(0, \sigma_h^2)$. We compute the expected pairwise probability of error and the expected overall probability of error at high SNR, and lower bounds for these. As SNR tends to infinity, the expected probability of error can be computed using the value of the density of minimum distance at zero [15]. Specifically, the expected pairwise probability of error can be computed from the PDF of minimum cluster distance at zero. To compute the PDF at zero, we consider ϵ-small regions in (h_1, h_2)-space around regions where minimum cluster distance is zero. In these regions, the minimum cluster distance is $d = |uh_1 + vh_2|$, where u and v are constants specific to each region and independent of h_1, h_2. The PDF at zero can be computed separately for these regions, which can be used to compute the overall PDF of minimum cluster distance at zero. In the case of expected overall probability of error, we use the same method, except that we consider the PDF of left and right minimum cluster distances instead of the PDF of minimum cluster distance.

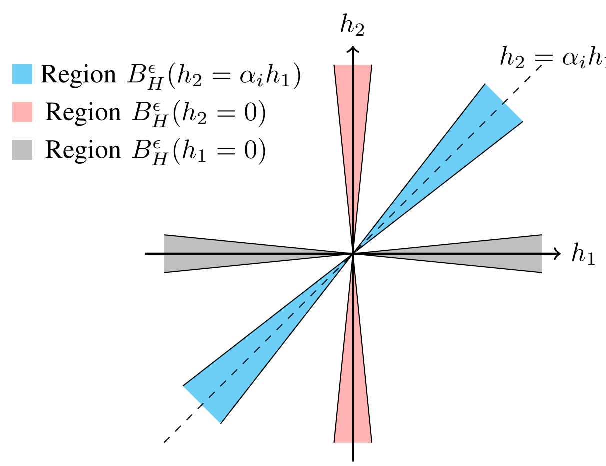

Fig. 7: Regions around $h_2 = \alpha_i h_1, h_2 = 0$ and $h_1 = 0$.

A. Distribution of minimum cluster distance

Consider the standard M-PAM constellation $\mathcal{A} = \{-(M-1), -(M-3), \cdots (M-1)\}$ with M being a power of 2. We assume that the regions Λ_i and the corresponding network maps f_i are given. Let $\mathbf{D}$ be the random variable corresponding to the minimum cluster distance $d(f, h_1, h_2)$, and $f_{\mathbf{D}}(\cdot)$ denote its PDF. To compute $\lim_{d\to 0} f_{\mathbf{D}}(d)$, we consider the following method.

Minimum cluster distance $d(f, h_1, h_2)$ can be 0 in the following three cases: (i) $\frac{h_2}{h_1} = \alpha_i, i \in$ NRI, $h_1, h_2 \neq 0$, (ii) $h_2 = 0$, and (iii) $h_1 = 0$. We consider the regions (i) $B_H^\epsilon(h_2 = \alpha_i h_1)$ around $h_2 = \alpha_i h_1, i \in$ NRI, (ii) $B_H^\epsilon(h_1 = 0)$ around $h_1 = 0$, and (iii) $B_H^\epsilon(h_2 = 0)$ around $h_2 = 0$, in $\mathbb{R}^2$ such that the following properties are satisfied:

1) $\{(h_1, h_2) : h_2 = \alpha_i h_1\} \subset B_H^\epsilon(h_2 = \alpha_i h_1) \subset \Lambda_i, i \in$ NRI,
2) $\{(h_1, h_2) : h_1 = 0\} \subset B_H^\epsilon(h_1 = 0) \subset \Lambda_{L+1}$,
3) $\{(h_1, h_2) : h_2 = 0\} \subset B_H^\epsilon(h_2 = 0) \subset \Lambda_{L+2}$.
4) $B_H^\epsilon(h_2 = \alpha_i h_1)$ is symmetric with respect to $h_2 = \alpha_i h_1$,
5) $B_H^\epsilon(h_1 = 0)$ is symmetric with respect to $h_1 = 0$,
6) $B_H^\epsilon(h_2 = 0)$ is symmetric with respect to $h_2 = 0$.

As a consequence of the first three conditions, the minimum cluster distance for each of these regions is of the form $|uh_1 + vh_2|$ where the constants $u, v \in \mathbb{Z}$ are specific to each region. So, we find the PDF of minimum cluster distance at zero, separately for these regions, and use it to compute the overall PDF of minimum cluster distance at zero. The last three conditions based on symmetry are useful for computing the PDF of minimum cluster distance at zero for each region. Next, we consider each region separately, and compute the PDF at zero.

1) Region $B_H^\epsilon(h_2 = \alpha_i h_1), i \in NRI$: Consider the singular fading state $\alpha_i, i \in$ NRI. For values of (h_1, h_2) such that $\frac{h_2}{h_1} = \alpha_i$, we have $\alpha_i h_1 - h_2 = 0$. So, to the singular fading state $\alpha_i, i \in$ NRI, we associate the region $S_{Hi} = \{(h_1, h_2) : \alpha_i h_1 - h_2 = 0\}$. Let us define

$$B_H^\epsilon(h_2 = \alpha_i h_1) = \left\{(h_1, h_2) : \alpha_i - \epsilon \leq \frac{h_2}{h_1} \leq \alpha_i + \epsilon\right\},$$

where $\epsilon > 0$ is small enough such that $B_H^\epsilon(h_2 = \alpha_i h_1) \subset \Lambda_i$. We see that $B_H^\epsilon(h_2 = \alpha_i h_1)$ satisfies the conditions that were stated earlier. The minimum cluster distance in the region $B_H^\epsilon(h_2 = \alpha_i h_1)$ is given by the expression

$$d(f_i, h_1, h_2) = |w_{1i} h_1 + w_{2i} h_2|,$$

where $w_{1i}, w_{2i} \neq 0$ are of the form

$$w_{1i} = x_{1i} - x'_{1i}, \tag{4}$$

$$w_{2i} = x_{2i} - x'_{2i}. \tag{5}$$

for some $(x_{1i}, x_{2i}), (x'_{1i}, x'_{2i}) \in \mathcal{A}^2, x_{1i} \neq x'_{1i}, x_{2i} \neq x'_{2i}$. Let E_{Hi} be the event that $(h_1, h_2) \in B_H^\epsilon(h_2 = \alpha_i h_1)$, and let $P_{Hi} = \Pr(E_{Hi})$. The PDF of minimum cluster distance in this region, at zero, is given as (derived in VI-A)

$$\lim_{d\to 0} f_{\mathbf{D}}(d|E_{Hi}) = \frac{1}{\sigma_h P_{Hi}} \sqrt{\frac{2}{\pi}} \frac{1}{\sqrt{w_{1i}^2 + w_{2i}^2}}, \ i \in \text{NRI}. \tag{6}$$

2) Region $B_H^\epsilon(h_2 = 0)$: Let us define

$$B_H^\epsilon(h_2 = 0) = \left\{(h_1, h_2) : -\epsilon \leq \frac{h_2}{h_1} \leq \epsilon\right\},$$

where $\epsilon < \frac{1}{M}$. The minimum cluster distance in this region for a given (h_1, h_2) is of the form $2|h_2|$ (derived in III-D1). We see that the region $B_H^\epsilon(h_2 = 0)$ satisfies the conditions that were stated earlier. Let E_{h_2} be the event that $(h_1, h_2) \in B_H^\epsilon(h_2 = 0)$, and let $P_{h_2} = \Pr(E_{h_2})$. The PDF of minimum cluster distance in this region, at zero, is given as (derived in VI-B)

$$\lim_{d\to 0} f_{\mathbf{D}}(d|E_{h_2}) = \frac{1}{\sigma_h \sqrt{2\pi} P_{h_2}}. \tag{7}$$

3) Region $B_H^\epsilon(h_1 = 0)$: Let us define

$$B_H^\epsilon(h_1 = 0) = \left\{(h_1, h_2) : -\epsilon \leq \frac{h_1}{h_2} \leq \epsilon\right\},$$

where $\epsilon < \frac{1}{M}$. The minimum cluster distance in this region for a given (h_1, h_2) is of the form $2|h_1|$ (refer section III-D1). Let E_{h_1} be the event that $(h_1, h_2) \in B_H^\epsilon(h_1 = 0)$, and let $P_{h_1} = \Pr(E_{h_1})$. Similar to the previous case, we can derive the following.

$$\lim_{d\to 0} f_{\mathbf{D}}(d|E_{h_1}) = \frac{1}{\sigma_h \sqrt{2\pi} P_{h_1}}. \tag{8}$$

The overall PDF of the minimum cluster distance is given by the expression

$$f_{\mathbf{D}}(d) = \sum_{i\in \text{NRI}} P_{Hi} f_{\mathbf{D}}(d|E_{Hi}) + P_{h_1} f_{\mathbf{D}}(d|E_{h_1}) + P_{h_2} f_{\mathbf{D}}(d|E_{h_2}) + P' f_{\mathbf{D}}(d|E_H^c),$$

where $P' = 1 - \sum_{i\in\text{NRI}} P_{Hi} - P_{h_1} - P_{h_2}$, and E_H^c is the event $(h_1, h_2) \notin B' = \left(\bigcup_{i\in\text{NRI}} B_H^\epsilon(h_2 = \alpha_i h_1)\right) \cup B_H^\epsilon(h_1 = 0) \cup B_H^\epsilon(h_2 = 0)$. Applying the limit $d \to 0$, we have

$$\lim_{d\to 0} f_{\mathbf{D}}(d) = \sum_{i\in\text{NRI}} \lim_{d\to 0} P_{Hi} f_{\mathbf{D}}(d|E_{Hi}) + \lim_{d\to 0} P_{h_1} f_{\mathbf{D}}(d|E_{h_1}) + \lim_{d\to 0} P_{h_2} f_{\mathbf{D}}(d|E_{h_2}) + \lim_{d\to 0} P' f_{\mathbf{D}}(d|E_H^c).$$

Since the minimum cluster distance is non-zero for all $(h_1, h_2) \notin B'$, the last term of the right-hand side expression reduces to 0. We have

$$\lim_{d\to 0} f_{\mathbf{D}}(d) = \frac{1}{\sigma_h}\sqrt{\frac{2}{\pi}} \left(\sum_{i\in\text{NRI}} \frac{1}{\sqrt{w_{1i}^2 + w_{2i}^2}} + 1\right).$$

Let $\mathbf{D_{jL}}$ be the random variable corresponding to the left minimum cluster distance $d_{jL}(f, h_1, h_2)$, and $f_{\mathbf{D_{jL}}}(\cdot)$ denote its PDF. Similar to the computation of the distribution of minimum cluster distance $f_{\mathbf{D}}$ at zero in the region $B_H^\epsilon(h_2 = \alpha_i h_1), i \in$ NRI, we can compute the distribution of left minimum cluster distance $f_{\mathbf{D_{jL}}}$ at zero in this region. We assume that the left minimum cluster distance with reference to (x_{1j}, x_{2j}) in the region $B_H^\epsilon(h_2 = \alpha_i h_1), i \in \text{NRIL}(j)$ is of the form $d_{jL}(f_i, h_1, h_2) = |w_{(1i,jL)} h_1 + w_{(2i,jL)} h_2|$, where the constants $w_{(1i,jL)} = x_{1i} - x'_{1i} > 0$, $x_{1i}, x'_{1i}, \in \mathcal{A}$ and $w_{(2i,jL)} = x_{2i} - x'_{2i} > 0$, $x_{2i}, x'_{2i} \in \mathcal{A}$ are specific to this region. We have,

$$\lim_{d\to 0} f_{\mathbf{D_{jL}}}(d|E_{Hi}) = \frac{1}{\sigma_h P_{Hi}} \sqrt{\frac{2}{\pi}} \frac{1}{\sqrt{w_{(1i,jL)}^2 + w_{(2i,jL)}^2}}, \quad i \in \text{NRIL}(j). \tag{9}$$

Similarly, let $\mathbf{D_{jR}}$ be the random variable corresponding to the right minimum cluster distance $d_{jR}(f, h_1, h_2)$, and $f_{\mathbf{D_{jR}}}(\cdot)$

denote its PDF. We have,

$$\lim_{d\to 0} f_{\mathbf{D_{jR}}}(d|E_{Hi}) = \frac{1}{\sigma_h P_{Hi}}\sqrt{\frac{2}{\pi}}\frac{1}{\sqrt{w^2_{(1i,jR)}+w^2_{(2i,jR)}}},\quad i\in \text{NRIR}(j). \tag{10}$$

B. Expected Pairwise Probability of Error

Theorem 1. *If nodes A and C use a M-PAM constellation $\mathcal{A}=\{-(M-1),-(M-3),\cdots(M-1)\}$, with channel coefficients $h_1,h_2\sim\mathcal{N}(0,\sigma_h^2)$, the expected pairwise probability of error in decoding any network-coded combination at the relay in the limit $SNR\to\infty$ is given as*

$$\lim_{SNR\to\infty} E[P_e] = \frac{F_P\sqrt{E_s}}{\sqrt{SNR}}\int_0^\infty Q\left(\frac{t}{2}\right)dt, \tag{11}$$

where E_s is the average energy in $\mathcal{A}$, F_P depends on the set of network maps chosen, and is given as

$$F_P = \sqrt{\frac{2}{\pi}}\left(\sum_{i\in NRI}\frac{1}{\sqrt{w_{1i}^2+w_{2i}^2}}+1\right). \tag{12}$$

The expected pairwise probability of error is given as

$$E[P_e]=\int_0^\infty Q\left(\frac{x}{2\sigma_N}\right)f_{\mathbf{D}}(x)dx,$$

where σ_N^2 is the noise-variance at the relay. Let $t=\frac{x}{\sigma_N}$. We have $dx=\sigma_N dt$. Then,

$$E[P_e]=\int_0^\infty Q\left(\frac{t}{2}\right)f_{\mathbf{D}}(\sigma_N t)\sigma_N dt.$$

Dividing both sides by σ_N, and applying the limit $\sigma_N\to 0$, we have

$$\begin{aligned}\lim_{\sigma_N\to 0}\frac{E[P_e]}{\sigma_N} &= \lim_{\sigma_N\to 0}\int_0^\infty Q\left(\frac{t}{2}\right)f_{\mathbf{D}}(\sigma_N t)dt,\\ &=\int_0^\infty Q\left(\frac{t}{2}\right)\lim_{\sigma_N\to 0}f_{\mathbf{D}}(\sigma_N t)dt,\\ &=\frac{F_P}{\sigma_h}\int_0^\infty Q\left(\frac{t}{2}\right)dt,\end{aligned}$$

where F_P is given by (12). We have

$$\lim_{\sigma_N\to 0}E[P_e]=\frac{F_P\sigma_N}{\sigma_h}\int_0^\infty Q\left(\frac{t}{2}\right)dt.$$

We define $SNR=\frac{E_s\sigma_h^2}{\sigma_N^2}$, where E_s is the average energy of the constellation $\mathcal{A}$. The limit $\sigma_N\to 0$ is equivalent to the limit $SNR\to\infty$. Therefore, we get (11). Since the expected pairwise error probability scales with $\frac{1}{\sqrt{SNR}}$, the diversity order is 0.5.

Remark: Performance of two different network mapping strategies can be compared by computing the constants $F_P^{(1)}$ and $F_P^{(2)}$ in (11). The SNR gain of network map 1 over network map 2 is seen to be $20\log_{10}\frac{F_P^{(1)}}{F_P^{(2)}}$ dB.

C. Approximate expected overall probability of error

Theorem 2. *If nodes A and C use a M-PAM constellation $\mathcal{A}=\{-(M-1),-(M-3),\cdots(M-1)\}$, with channel coefficients $h_1,h_2\sim\mathcal{N}(0,\sigma_h^2)$, the expected overall probability of error in decoding any network-coded combination at the relay in the limit $SNR\to\infty$ can be approximated as*

$$\lim_{SNR\to\infty}E[P_e']\approx\frac{F_P'\sqrt{Es}}{\sqrt{SNR}}\int_0^\infty Q\left(\frac{u}{2}\right)du, \tag{13}$$

where E_s is the average energy in $\mathcal{A}$, F_P' depends on the set of network maps chosen, and is given as

$$F_P' = \frac{1}{M^2}\sqrt{\frac{2}{\pi}}\left(\sum_{j=1}^{M^2}\left(\sum_{i\in NRIL(j)}\frac{1}{\sqrt{w^2_{(1i,jL)}+w^2_{(2i,jL)}}}+\sum_{i\in NRIR(j)}\frac{1}{\sqrt{w^2_{(1i,jR)}+w^2_{(2i,jR)}}}\right)+2M(M-1)\right). \tag{14}$$

Let us denote the overall probability of error in decoding the cluster at the relay at the given channel coefficients h_1,h_2 as $P_e'(h_1,h_2)$ (or simply P_e'). We can write the expected overall probability of error as

$$E[P_e']=\sum_{i=1}^{L}P_{Hi}E[P_e'|E_{Hi}]+P_{h_1}E[P_e'|E_{h_1}]+P_{h_2}E[P_e'|E_{h_2}]+P'E[P_e'|E_H^c],$$

where the events $E_{Hi},E_{h_1},E_{h_2},E_H^c$ and probabilities $P_{Hi},P_{h_1},P_{h_2},P'$ are as defined earlier. Dividing both sides by σ_N, and applying the limit $\sigma_N\to 0$, we have

$$\lim_{\sigma_N\to 0}\frac{E[P_e']}{\sigma_N}=\lim_{\sigma_N\to 0}\frac{1}{\sigma_N}\Big(\sum_{i=1}^{L}P_{Hi}E[P_e'|E_{Hi}]+P_{h_1}E[P_e'|E_{h_1}]+P_{h_2}E[P_e'|E_{h_2}]\Big). \tag{15}$$

Next, we compute $\lim_{\sigma_N\to 0}\frac{E[P_e'|E_{Hi}]}{\sigma_N}$. We can write

$$P_e'=\sum_{j=1}^{M^2}P'_{e|x_{1j},x_{2j}}\Pr(x_{1j},x_{2j}),$$

where $P'_{e|x_{1j},x_{2j}}$ is the error probability given the symbol pair (x_{1j},x_{2j}) is transmitted from nodes A and C, and $\Pr(x_{1j},x_{2j})$ is the probability that the pair (x_{1j},x_{2j}) is transmitted. Let us assume that every pair $(x_{1j},x_{2j})\in\mathcal{A}^2$ is equally likely with probability $\frac{1}{M^2}$. We can approximate $P'_{e|x_{1j},x_{2j}}\approx Q\left(\frac{d_{jL}}{2\sigma_N}\right)+Q\left(\frac{d_{jR}}{2\sigma_N}\right)$, where d_{jL} and d_{jR} are the left minimum cluster distance and right minimum cluster distance, respectively, with reference to (x_{1j},x_{2j}). We have

$$P_e'\approx\frac{1}{M^2}\sum_{j=1}^{M^2}Q\left(\frac{d_{jL}}{2\sigma_N}\right)+Q\left(\frac{d_{jR}}{2\sigma_N}\right).$$

Taking expectation conditioned on E_{Hi} both the sides, we have

$$E[P_e'|E_{Hi}]\approx\frac{1}{M^2}\sum_{j=1}^{M^2}E\left[Q\left(\frac{d_{jL}}{2\sigma_N}\right)\Big|E_{Hi}\right]+E\left[Q\left(\frac{d_{jR}}{2\sigma_N}\right)\Big|E_{Hi}\right].$$

Dividing both sides by σ_N, and applying the limit $\sigma_N\to 0$, we have

$$\lim_{\sigma_N\to 0}\frac{E[P_e'|E_{Hi}]}{\sigma_N}\approx\lim_{\sigma_N\to 0}\frac{1}{M^2\sigma_N}\sum_{j=1}^{M^2}E\left[Q\left(\frac{d_{jL}}{2\sigma_N}\right)\Big|E_{Hi}\right]+E\left[Q\left(\frac{d_{jR}}{2\sigma_N}\right)\Big|E_{Hi}\right],$$

$$= \frac{1}{M^2}\int_0^\infty Q\left(\frac{t}{2}\right)\Bigg(\sum_{j=1}^{M^2}\lim_{\sigma_N\to 0} f_{\mathbf{D_{jL}}}(\sigma_N t|E_{Hi}) + \lim_{\sigma_N\to 0} f_{\mathbf{D_{jR}}}(\sigma_N t|E_{Hi})\Bigg)dt.$$

The other conditional expectations in (15) can be derived using results from III-D2. Using these in (15), we have

$$\lim_{\sigma_N\to 0}\frac{E[P_e']}{\sigma_N} \approx \frac{F_P'}{\sigma_h}\int_0^\infty Q\left(\frac{t}{2}\right),$$

where F_P' is given by (14). Writing in terms of $SNR = \frac{E_s\sigma_h^2}{\sigma_N^2}$, we have (13).

Remark: From (11) and (13), we see that the expected error probabilities depend on the constants F_P and F_P'. In order to minimize the error probabilities, it is desirable to use network maps that can minimize these constants. Specifically, using network maps that have a large minimum cluster distance implies a smaller value for these constants, and thus minimize the error probabilities. It is optimal to use network maps that have $|\text{NRI}| = 0$. Even though we can construct ring-linear network maps to ensure $|\text{NRI}| = 0$, not all such maps are guaranteed to be valid. For this purpose, non-linear network maps could be considered, whose construction we discuss in our earlier work [14].

D. Lower bounds

In this section, we derive lower bounds on pairwise and overall error probabilities for any network map.

1) Pairwise error probability:

Theorem 3. *If nodes A and C use a M-PAM constellation $\mathcal{A} = \{-(M-1), -(M-3), \cdots (M-1)\}$, with channel coefficients $h_1, h_2 \sim \mathcal{N}(0,\sigma_h^2)$, the expected pairwise probability of error in decoding any network-coded combination at the relay in the limit $SNR \to \infty$ can be lower bounded as*

$$\lim_{SNR\to\infty} E[P_e] \geq \frac{\sqrt{E_s}}{\sqrt{SNR}}\sqrt{\frac{2}{\pi}}\int_0^\infty Q\left(\frac{t}{2}\right)dt. \quad (16)$$

The constant F_P in the expected pairwise probability of error is given as

$$\begin{aligned} F_P &= \lim_{d\to 0} f_{\mathbf{D}}(d)\sigma_h, \\ &= \sigma_h \sum_{i\in\text{NRI}} \lim_{d\to 0} P_{Hi} f_{\mathbf{D}}(d|E_{Hi}) \\ &\quad + \lim_{d\to 0} P_{h_1} f_{\mathbf{D}}(d|E_{h_1}) + \lim_{d\to 0} P_{h_2} f_{\mathbf{D}}(d|E_{h_2}). \end{aligned} \quad (17)$$

The expected pairwise probability of error can be minimized by minimizing F_P, which depends on the set of network maps $\{f_1, f_2, \cdots, f_{L+2}\}$ chosen. Specifically, if we choose the network maps such that $\text{NRI} = \{\phi\}$, the summation term in (17) reduces to zero, which minimizes F_P. The other two terms are non-zero irrespective of the set of network maps chosen. Hence, the minimum value of F_P is

$$F_P^{(\min)} = \lim_{d\to 0} P_{h_1} f_{\mathbf{D}}(d|E_{h_1})\sigma_h + \lim_{d\to 0} P_{h_2} f_{\mathbf{D}}(d|E_{h_2})\sigma_h.$$

Next, we characterize the minimum cluster distance in the regions $B_H^\epsilon(h_2 = 0)$ and $B_H^\epsilon(h_1 = 0)$, which are used to derive $F_P^{(\min)}$. Let us consider the region $B_H^\epsilon(h_2 = 0)$ in the neighborhood of $h_2 = 0$. Assume that the region is small enough that $|\frac{h_2}{h_1}| < \frac{1}{M}\ \forall\ (h_1, h_2) \in B_H^\epsilon(h_2 = 0)$. Let us consider the ordered subsets of transmit symbol pairs, $\lambda_1, \lambda_2, \cdots \lambda_M \subset \mathcal{A}^2$, where $\lambda_l = \{(2l-M-1, v_1), (2l-M-1, v_2), \cdots (2l-M-1, v_M)\}$. Here, $v_1, v_2 \cdots v_M \in \mathcal{A}$, $v_i \neq v_j$ are ordered such that $v_1 h_2 \leq v_2 h_2 \cdots \leq v_M h_2$. Let $T_1, T_2 \cdots T_M \subset \mathcal{M}_B$ be ordered subsets of points in the relay constellation $\mathcal{M}_B$, where $T_l = \{(2l-M-1)h_1 + v_1 h_2, (2l-M-1)h_1 + v_2 h_2, \cdots (2l-M-1)h_1 + v_M h_2\}$. We note that the points in T_l collapse to the point $(2l-M-1)h_1 \in \mathcal{M}_B$ at $h_2 = 0$. Also, the points in T_l are ordered according to their positions in $\mathcal{M}_B$ from left to right. It can be proved that, for a given $(h_1, h_2) \in B_H^\epsilon(h_2 = 0)$, the minimum distance between points in $\mathcal{M}_B$ is the distance between any two adjacent points in T_l, which is $\mu_{\min} = 2|h_2|$. This corresponds to transmit pairs of the form $(x_1, x_2), (x_1, x_2 \pm 2) \in \mathcal{A}^2$. The network map f_{L+2} associated with the region $B_H^\epsilon(h_2 = 0) \subset \Lambda_{L+2}$ needs to satisfy the Exclusive law as follows.

$$f_{L+2}(a,b) \neq f_{L+2}(a,b')\ \forall\ b \neq b', a, b, b' \in \mathcal{A}. \quad (18)$$

So, we have $f_{L+2}(x_1, x_2) \neq f_{L+2}(x_1, x_2 \pm 2)\ \forall\ x_1, x_2, (x_2 \pm 2) \in \mathcal{A}$. Since the pairs (x_1, x_2) and $(x_1, x_2 \pm 2)$ are network-mapped to different values, the minimum cluster distance in $\mathcal{M}_B$ in the region $(h_1, h_2) \in B_H^\epsilon(h_2 = 0)$ is $2|h_2|$, corresponding to transmit pairs of the form $(x_1, x_2), (x_1, x_2 \pm 2) \in \mathcal{A}^2$.

Similarly, we can prove that the minimum cluster distance in $\mathcal{M}_B$ in the region $B_H^\epsilon(h_1 = 0)$ is $2|h_1|$, and the corresponding transmit pairs are of the form $(x_1, x_2), (x_1 \pm 2, x_2) \in \mathcal{A}^2$.

Let $f_{\mathbf{D}}$ be the PDF of the random variable $\mathbf{D}$ corresponding to the minimum cluster distance $d = 2|h_1|$ (in the region $B_H^\epsilon(h_1 = 0)$), and $d = 2|h_2|$ (in the region $B_H^\epsilon(h_2 = 0)$). Substituting for $\lim_{d\to 0} f_{\mathbf{D}}(d|E_{h_1})$ (refer VI-B) and $\lim_{d\to 0} f_{\mathbf{D}}(d|E_{h_2})$, we have

$$F_P^{(\min)} = \sqrt{\frac{2}{\pi}}.$$

Irrespective of the network maps assigned to the regions $B_H^\epsilon(h_1 = 0)$ and $B_H^\epsilon(h_2 = 0)$, we have $\lim_{d\to 0} f_{\mathbf{D}} > 0$ for these regions. Thus, we have the lower bound (16) for the expected pairwise probability of error.

2) Overall error probability:

Theorem 4. *If nodes A and C use a M-PAM constellation $\mathcal{A} = \{-(M-1), -(M-3), \cdots (M-1)\}$, with channel coefficients $h_1, h_2 \sim \mathcal{N}(0,\sigma_h^2)$, the expected overall probability of error in decoding any network-coded combination at the relay in the limit $SNR \to \infty$ can be lower bounded as*

$$\lim_{SNR\to\infty} E[P_e'] \geq \frac{4(M-1)\sqrt{Es}}{\sqrt{2\pi}M\sqrt{SNR}}\int_0^\infty Q\left(\frac{u}{2}\right)du. \quad (19)$$

Similar to the case of pairwise error, the expected overall error probability can be minimized by choosing a set of network maps $\{f_1.f_2, \cdots f_{L+2}\}$ such that $\text{NRI} = \{\phi\}$. Then, we have

$$\lim_{\sigma_N\to 0}\frac{E[P_e']}{\sigma_N}^{(\min)} = \lim_{\sigma_N\to 0} P_{h_1}\frac{E[P_e'|E_{h_1}]}{\sigma_N} + P_{h_2}\frac{E[P_e'|E_{h_2}]}{\sigma_N}. \quad (20)$$

We first compute $\lim_{\sigma_N\to 0}\frac{1}{\sigma_N}E[P_e'|E_{h_2}]$ in the right-hand side expression. Let $P'_{e|(l,p)}$ denote the overall probability of error in decoding at the relay, given the transmit symbol pair $(2l-M-1, v_p) \in \Lambda_l$. We can write $P'_{e|(l,p)} = Q\left(\frac{d_{L(l,p)}}{2\sigma_N}\right) + Q\left(\frac{d_{R(l,p)}}{2\sigma_N}\right)$, where $d_{L(l,p)}$ and $d_{R(l,p)}$ are the left and right

This is the author's version of an article that has been published in this journal. Changes were made to this version by the publisher prior to publication.
The final version of record is available at http://dx.doi.org/10.1109/TCOMM.2017.2657756

minimum cluster distances, respectively, with reference to $(2l-M-1, v_p)$. Let $\mathbf{D_{L(l,p)}}$ and $\mathbf{D_{R(l,p)}}$ denote the random variables corresponding to $d_{L(l,p)}$ and $d_{R(l,p)}$, respectively. We have

$$E[P_e'|E_{h_2}] = \frac{1}{M^2}\sum_{l=1}^{M}\sum_{p=1}^{M} E[P'_{e|(l,p)}|E_{h_2}],$$
$$= \frac{1}{M^2}\sum_{l=1}^{M}\sum_{p=1}^{M}\int_0^{\infty} Q\left(\frac{t}{2\sigma_N}\right) f_{\mathbf{D_{L(l,p)}}}(t|E_{h_2})dt$$
$$+ \int_0^{\infty} Q\left(\frac{t}{2\sigma_N}\right) f_{\mathbf{D_{R(l,p)}}}(t|E_{h_2})dt,$$

where $f_{\mathbf{D_{L(l,p)}}}$ and $f_{\mathbf{D_{R(l,p)}}}$ denote the PDFs of $\mathbf{D_{L(l,p)}}$ and $\mathbf{D_{R(l,p)}}$, respectively. Dividing both sides by σ_N^2, and applying the limit $\sigma_N \to 0$, we have

$$\lim_{\sigma_N\to 0}\frac{E[P_e'|E_{h_2}]}{\sigma_N} =$$
$$\frac{1}{M^2}\int_0^{\infty} Q\left(\frac{u}{2}\right)\left(\lim_{\sigma_N\to 0}\sum_{l=1}^{M}\sum_{p=1}^{M} f_{\mathbf{D_{L(l,p)}}}(\sigma_N u|E_{h_2})\right.$$
$$\left. + f_{\mathbf{D_{R(l,p)}}}(\sigma_N u|E_{h_2})\right)du.$$

The expressions for $\lim_{d\to 0} f_{\mathbf{D_{L(l,p)}}}(d|E_{h_2})$ and $\lim_{d\to 0} f_{\mathbf{D_{R(l,p)}}}(d|E_{h_2})$ are derived in VI-C. Using them, we get

$$\lim_{\sigma_N\to 0}\frac{E[P_e'|E_{h_2}]}{\sigma_N} = \frac{M-1}{\sigma_h P_{h_2} M}\sqrt{\frac{2}{\pi}}\int_0^{\infty} Q\left(\frac{u}{2}\right)du.$$

Similarly, deriving $\lim_{\sigma_N\to 0}\frac{E[P_e'|E_{h_1}]}{\sigma_N}$ and substituting in (20), we get

$$\lim_{\sigma_N\to 0}\frac{E[P_e']^{(\min)}}{\sigma_N} = \frac{4(M-1)}{\sigma_h M\sqrt{2\pi}}\int_0^{\infty} Q\left(\frac{u}{2}\right)du.$$

In terms of $SNR = \frac{E_s\sigma_h^2}{\sigma_N^2}$, we have the lower bound (19).

IV. M^2-QAM

In this section we consider the case of $\mathcal{A}$ being M^2-QAM, and channel coefficients (h_1, h_2) being *iid* $\mathcal{CN}(0,\sigma_h^2)$. We compute the expected pairwise probability of error at high SNR, and a lower bounds for this. The expected pairwise probability of error in the limit SNR tends to infinity can be computed from the PDF of minimum cluster distance vector at zero. For this, we consider regions as in the case of M-PAM, and compute the PDF at zero separately for each region. This can be used to compute the overall PDF of minimum cluster distance vector at zero. Since the analysis is mostly similar to the case of M-PAM, we only outline the method, and provide the final expressions.

A. Distribution of minimum cluster distance

Consider the standard M^2-QAM constellation $\mathcal{A} = \{u+iv : u,v \in \{-(M-1), -(M-3), \cdots (M-1)\}\}$ with M being a power of 2. Let $h_1 = h_{R1}+ih_{I1}, h_2 = h_{R2}+ih_{I2}$, where the variances of $h_{R1}, h_{I1}, h_{R2}, h_{I2}$ are $\frac{\sigma_h^2}{2}$ each. Let $\mathbf{D}$ be the random vector corresponding to the minimum cluster distance vector $D = [d_R \quad d_I]$. Let $f_{\mathbf{D}}(\cdot)$ denote the PDF of $\mathbf{D}$. As in the case of M-PAM, to compute $\lim_{\substack{d_R\to 0\\ d_I\to 0}} f_{\mathbf{D}}(d_R, d_I)$, we consider the following method. Minimum cluster distance $d(f, h_1, h_2)$ can be 0 in the following three cases: (1) $\frac{h_2}{h_1} = \alpha_i, i \in$ NRI, $h_1, h_2 \neq 0$, (2) $h_2 = 0$, and (3) $h_1 = 0$. As in the case of M-PAM, we consider the regions (i) $B_H^{\epsilon}(h_2 = \alpha_i h_1), i \in$ NRI, (ii) $B_H^{\epsilon}(h_1 = 0)$, and (iii) $B_H^{\epsilon}(h_2 = 0)$ in $\mathbb{R}^4$ that satisfy the following properties.

1) $\{(h_{R1}, h_{I1}, h_{R2}, h_{I2}) \in \mathbb{R}^4 : \frac{h_{R2}+ih_{I2}}{h_{R1}+ih_{I1}} = \alpha_i\} \subset B_H^{\epsilon}(h_2 = \alpha_i h_1) \subset \Lambda_i, i \in$ NRI,
2) $\{(h_{R1}, h_{I1}, h_{R2}, h_{I2}) \in \mathbb{R}^4 : h_{R1}, h_{I1} = 0\} \subset B_H^{\epsilon}(h_1 = 0) \subset \Lambda_{L+1}$,
3) $\{(h_{R1}, h_{I1}, h_{R2}, h_{I2}) \in \mathbb{R}^4 : h_{R2}, h_{I2} = 0\} \subset B_H^{\epsilon}(h_2 = 0) \subset \Lambda_{L+2}$.

The minimum cluster distance vector in these regions are of the form $D = [|\Re\{c_1h_1 + c_2h_2\}| \; |\Im\{c_1h_1 + c_2h_2\}|]$ where the constants $c_1, c_2 \in \mathbb{C}$ are specific to each region. So, PDF of minimum cluster distance vector at zero can be found separately for these regions, and used to compute the overall PDF of minimum cluster distance vector at zero. We can show that

$$\lim_{\substack{d_R\to 0\\ d_I\to 0}} f_{\mathbf{D}}(d_R, d_I) = \frac{4}{\pi\sigma_h^2}\left(\sum_{i\in \text{NRI}}\frac{1}{|w_{1i}|^2 + |w_{2i}|^2} + \frac{1}{2}\right).$$

B. Expected pairwise Probability of Error

Theorem 5. *If nodes A and C use a M^2-QAM constellation $\mathcal{A} = \{u+iv : u,v \in \{-(M-1), -(M-3), \cdots (M-1)\}\}$, with channel coefficients $h_1, h_2 \sim \mathcal{CN}(0,\sigma_h^2)$, the expected pairwise probability of error in decoding any network-coded combination at the relay in the limit $SNR \to \infty$ is given as*

$$\lim_{SNR\to\infty} E[P_e] = \frac{\pi}{4}\frac{F_Q E_s}{SNR}\int_0^{\infty} rQ\left(\frac{r}{2}\right)dr, \tag{21}$$

where E_s is the average energy in $\mathcal{A}$, F_Q depends on the set of network maps chosen, and is given by (22)

The expected pairwise probability of error is given by the expression

$$E[P_e] = \int_0^{\infty}\int_0^{\infty} Q\left(\frac{\sqrt{x^2+y^2}}{2\sigma_N}\right) f_{\mathbf{D}}(x,y)dxdy.$$

Let $x = \sigma_N r\cos\theta$ and $y = \sigma_N r\sin\theta$. Then, we have

$$E[P_e] = \sigma_N^2\int_0^{\infty}\int_0^{\frac{\pi}{2}} Q\left(\frac{r}{2}\right) f_{\mathbf{D}}(\sigma_N r\cos\theta, \sigma_N r\sin\theta)rd\theta dr.$$

Dividing both sides by σ_N^2, and applying the limit $\sigma_N \to 0$, we can show that

$$\lim_{\sigma_N\to 0} E[P_e] = \frac{\pi}{2}\frac{F_Q\sigma_N^2}{\sigma_h^2}\int_0^{\infty} rQ\left(\frac{r}{2}\right)dr.$$
$$F_Q = \lim_{\substack{d_R\to 0\\ d_I\to 0}} f_{\mathbf{D}}(d_R, d_I)\sigma_h^2,$$
$$= \frac{4}{\pi}\left(\sum_{i\in\text{NRI}}\frac{1}{|w_{1i}|^2 + |w_{2i}|^2} + \frac{1}{2}\right). \tag{22}$$

In terms of $SNR = \frac{E_s\sigma_h^2}{2\sigma_N^2}$, we have (21).

C. Lower bound on expected pairwise error probability

In this section, we derive a lower bound on pairwise error probability for any network map.

This is the author's version of an article that has been published in this journal. Changes were made to this version by the publisher prior to publication.
The final version of record is available at http://dx.doi.org/10.1109/TCOMM.2017.2657756

Theorem 6. *If nodes A and C use a M^2-QAM constellation $\mathcal{A} = \{u + iv : u, v \in \{-(M-1), -(M-3), \cdots (M-1)\}\}$, with channel coefficients $h_1, h_2 \sim \mathcal{CN}(0, \sigma_h^2)$, the expected pairwise probability of error in decoding any network-coded combination at the relay in the limit $SNR \to \infty$ can be lower bounded as*

$$E[P_e] \geq \frac{E_s}{2SNR} \int_0^\infty rQ\left(\frac{r}{2}\right) dr. \tag{23}$$

The expected pairwise probability of error is given by the expression (from (21))

$$\lim_{SNR \to \infty} E[P_e] = \frac{\pi}{4} \frac{F_Q E_s}{SNR} \int_0^\infty rQ\left(\frac{r}{2}\right) dr,$$

where

$$F_Q = \sigma_h^2 \sum_{i \in \text{NRI}} \lim_{\substack{d_R \to 0 \\ d_I \to 0}} P_{Hi} f_{\mathbf{D}}(d_R, d_I | E_{Hi}) + \lim_{\substack{d_R \to 0 \\ d_I \to 0}} P_{h_1} f_{\mathbf{D}}(d_R, d_I | E_{h_1}) + \lim_{\substack{d_R \to 0 \\ d_I \to 0}} P_{h_2} f_{\mathbf{D}}(d_R, d_I | E_{h_2}). \tag{24}$$

The expected pairwise probability of error can be minimized by minimizing F_Q, which depends on the set of network maps $\{f_1, f_2, \cdots, f_{L+2}\}$ chosen. Specifically, if we choose the network maps such that NRI $= \{\phi\}$, the summation term in (24) reduces to zero, which minimizes F_Q. The other two terms are non-zero irrespective of the set of network maps chosen. Hence, the minimum value of F_Q is

$$F_Q^{(\min)} = \lim_{\substack{d_R \to 0 \\ d_I \to 0}} P_{h_1} f_{\mathbf{D}}(d_R, d_I | E_{h_1}) \sigma_h^2 + \lim_{\substack{d_R \to 0 \\ d_I \to 0}} P_{h_2} f_{\mathbf{D}}(d_R, d_I | E_{h_2}) \sigma_h^2.$$

The corresponding minimum expected pairwise probability of error is

$$\lim_{SNR \to \infty} E[P_e]^{(\min)} = \frac{\pi}{4} \frac{F_Q^{(\min)} E_s}{SNR} \int_0^\infty rQ\left(\frac{r}{2}\right) dr. \tag{25}$$

This also gives us a lower bound for the expected pairwise probability of error. We can show that $F_Q = \frac{2}{\pi}$. This can be derived using a method similar to that used for deriving F_P in section III-D1. Substituting for F_Q in (25), we have the lower bound (23).

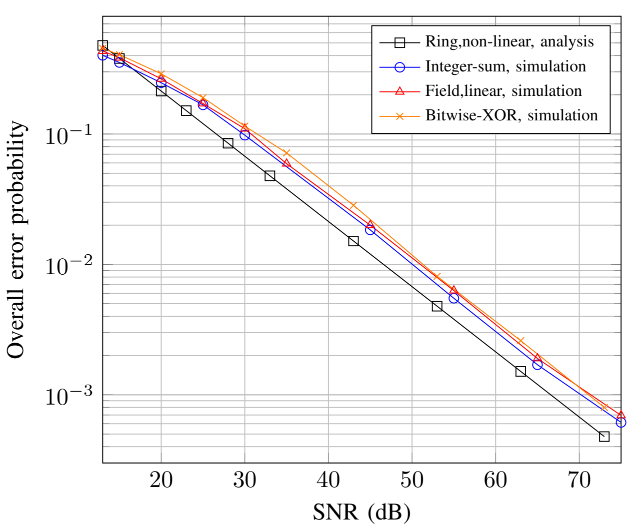

Fig. 8: Overall error probability- 4-PAM.

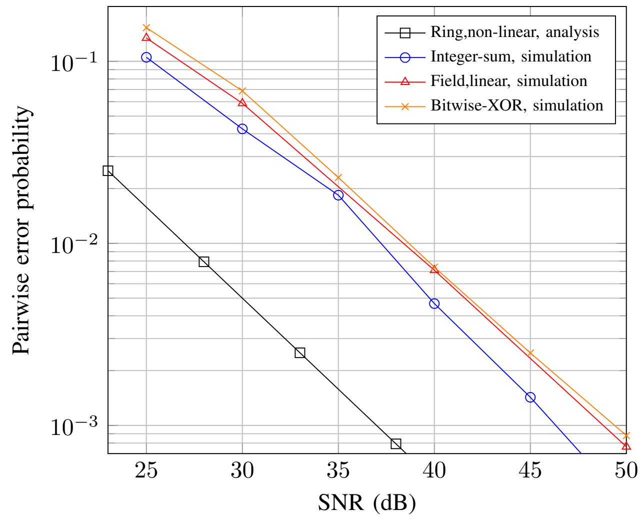

Fig. 9: Pairwise error probability- 16-QAM.

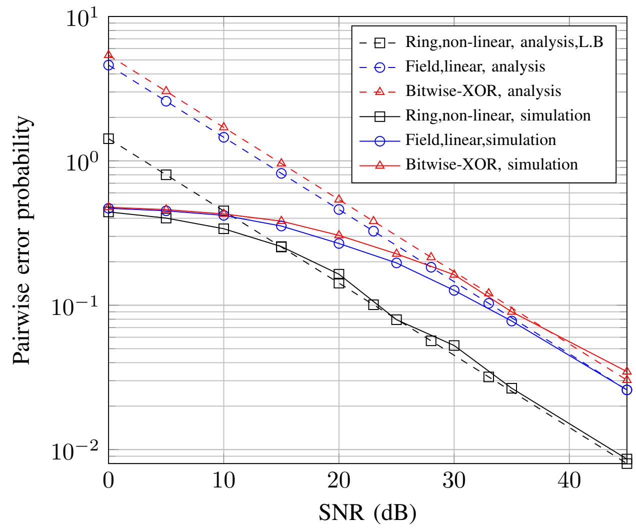

Fig. 10: Pairwise error probability- 4-PAM.

V. Simulation Results

A. Comparison with other schemes

In this section, we compare error performance of ring-based non-linear network mapping strategy with some of the earlier strategies: (i) Integer-sum based linear network mapping strategy [17] (ii) Field based linear network mapping strategy [16] (iii) Bitwise-XOR based network mapping strategy [11].

In the ring based network mapping strategy, we consider a set of network maps $\mathcal{F}_R = \{f_1^R, f_2^R, \cdots f_{L+2}^R\}$, of which each map f_i^R is a linear or non-linear network map over the ring $\mathbb{Z}_4 = \{0, 1, 2, 3\}$ for 4-PAM and over the ring $\mathbb{Z}_4[i] = \{u + iv : u, v \in \mathbb{Z}_4\}$ for 16-QAM. The set of network maps $\mathcal{F}_R$ is chosen such that NRI $= \{\phi\}$. In the Integer-sum based network mapping strategy [17], we consider a set of network maps $\mathcal{F}_I = \{f_1^I, f_2^I, \cdots f_{L+2}^I\}$, of which each map f_i^I is a linear network map over $\mathbb{Z}_4 = \{0, 1, 2, 3\}$ for 4-PAM and over $\mathbb{Z}_{16} = \{0, 1, \cdots 15\}$ for 16-QAM. In the field based network mapping strategy [16], we consider a set of network maps $\mathcal{F}_F = \{f_1^F, f_2^F, \cdots f_{L+2}^F\}$, of which each map f_i^F is a linear network map over the field $\mathbb{F}_4$ for 4-PAM and over the field $\mathbb{F}_{16}$ for 16-QAM. In the XOR based clustering strategy [11], we consider a single network map f_{XOR} that corresponds to decoding the bit-wise XOR of the transmit symbols. For the ring-based strategy, network maps from $\mathcal{F}_R$ are assigned to different regions in (h_1, h_2)-space, as described in section II. For the other strategies, the network map for a given h_1, h_2 is chosen based on a distance criterion as suggested in [11].

We consider a block fading channel with channel coefficients $h_1, h_2 \sim \mathcal{N}(0, \sigma_h^2)$ for 4-PAM transmit constellation and $h_1, h_2 \sim \mathcal{CN}(0, \sigma_h^2)$ for 16-QAM transmit constellation. In Figure 8, we consider a 4-PAM transmit constellation and plot the expected overall error probabilities for ring-based strategy at different SNRs. These are based on the expression (13). For comparison, we plot the overall symbol error rates at the relay for integer-sum based, field based and bitwise-XOR based strategies, obtained using simulation as follows. We transmit blocks of N symbols form nodes A and C, and determine the number of symbol errors after estimating the network-mapped symbols at the relay. A block is considered to be in error if there is at least one symbol error. We count up to 100 block errors to compute the symbol error rate. As seen from the Figure, we note that the error performance of ring-based non-linear strategy is better than that for all the other strategies. This is because, the ring-based strategy considers both linear and non-linear maps unlike the other strategies, which results in larger distances between points from different clusters in the relay constellation.

In Figure 9, we consider a 16-PAM transmit constellation and plot the expected pairwise error probabilities for ring-based strategy at different SNRs. These are based on the expression (21). For comparison, we plot the pairwise symbol error rates at the relay for integer-sum based, field based and bitwise-XOR based strategies, obtained using simulation as follows. We transmit blocks of N symbols from nodes A and C. For each block, the minimum cluster distance $d_{\min}^C$ is computed using (1) from the values of h_1, h_2 and the network map chosen. For determining the pairwise symbol error rate, we consider a binary-input additive white Gaussian channel: $y = x + n$, where $x \in \left\{-\frac{d_{\min}^C}{2}, \frac{d_{\min}^C}{2}\right\}$, $n \sim \mathcal{CN}(0, 2\sigma_N^2)$ for 16-QAM. For each transmit block we determine the number of symbol errors after estimating these transmitted symbols from the received values of the channel. We count up to 500 block errors for to compute the pairwise symbol error rate. As seen from the Figure, we note that the error performance of ring-based non-linear network mapping strategy is better than that of all the other strategies. The ring-based non-linear network mapping strategy requires the construction of non-linear network maps, which results in additional complexity. However, this may be done off-line using methods proposed in our earlier work [14].

B. Comparison of results from analysis with simulated results

In this section, we consider a M-PAM transmit constellation and compare the error performance results obtained from analysis and simulation for the each of the following network mapping strategies: (i) Ring-based non-linear network mapping strategy (ii) Field based linear network mapping strategy (iii) Bitwise-XOR based network mapping strategy. Specifically, we plot in Figure 10 expected pairwise error probabilities (using (11)) and pairwise symbol error rates (based on simulation) at different SNRs. The expected pairwise error probability plot for the ring-based network mapping strategy also forms the lower bound, since in this case $|\mathrm{NRI}| = 0$. For the ring based, field based and XOR based strategies, we consider sets of network maps denoted $\mathcal{F}_R$, $\mathcal{F}_F$ and $\mathcal{F}_{XOR}$, respectively, and choose a map for a given h_1, h_2 from these sets based on the method described in section II. From the plots we see that for $SNR > 30$ dB, the results obtained using analysis are close to the simulated results.

VI. Conclusion

In this work, we considered a bidirectional relaying setup and characterized the error performance in decoding the network-coded combination at the relay at high SNR. Specifically, we derived expressions for the expected pairwise error probability (with M-PAM and M^2-QAM transmit constellations) and approximate expected overall error probability (with M-PAM transmit constellation). Also, we derived lower bounds for these. Using the expressions for error probability, we compare the error performance of ring based non-linear network mapping strategy with other network mapping strategies such as field based and bitwise-XOR based strategies. Based on the results obtained, we find that the ring based strategy is better than the other strategies. This is consistent with the simulated results and also with the results from our earlier work.

Appendix

A. PDF of minimum cluster distance in the region $B_H^\epsilon(h_2 = \alpha_i h_1)$ for M-PAM

Let us consider the linear transformation

$$y_1 = w_{1i}h_1 + w_{2i}h_2, \tag{26}$$
$$y_2 = h_2. \tag{27}$$

Since $w_{1i}, w_{2i} > 0 \,\forall\, i \in \mathrm{NRI}$, this transformation is always invertible. This transformation maps the region $B_H^\epsilon(h_2 = \alpha_i h_1)$ to the region $B_{Yi} = \{(y_1, y_2) : A_i^{-1} Y^T \in B_H^\epsilon(h_2 = \alpha_i h_1)\}$, where $A_i = \left[\begin{smallmatrix} w_{1i} & w_{2i} \\ 0 & 1 \end{smallmatrix}\right]$, and $Y = [y_1\, y_2]$. Let E_{Yi} be the event that $(y_1, y_2) \in B_{Yi}$. We note that the events E_{Hi} and E_{Yi} are equivalent since there is an one-to-one mapping between the regions $B_H^\epsilon(h_2 = \alpha_i h_1)$ and B_{Yi} (equations (26), (27)). Let $\mathbf{Y}$ and $\mathbf{H}$ be the random vectors corresponding to $Y = [y_1\, y_2]$ and $H = [h_1\, h_2]$, respectively. The PDF of $\mathbf{H}$ conditioned on the event E_{Hi} is computed as

$$f_{\mathbf{H}}(h_1, h_2 | E_{Hi}) = \frac{1}{2\pi\sigma_h^2 P_{Hi}} \exp\left(-\frac{h_1^2 + h_2^2}{2\sigma_h^2}\right),$$
$$(h_1, h_2) \in B_H^\epsilon(h_2 = \alpha_i h_1), \tag{28}$$

where $P_{Hi} = \Pr(E_{Hi})$. The PDF of $\mathbf{Y}$ conditioned on the event E_{Yi} can be computed as

$$f_{\mathbf{Y}}(Y | E_{Yi}) = |J(Y)| f_{\mathbf{H}}(A_i^{-1} Y^T | E_{Hi}),$$

where $|J(Y)| = \frac{1}{|w_{1i}|}$ is the determinant of Jacobian matrix corresponding to the linear transformation. The PDF of the random variable $\mathbf{Y_1}$ corresponding to y_1 can be computed by marginalizing the PDF of $\mathbf{Y}$ as follows.

$$f_{\mathbf{Y_1}}(y_1|E_{Yi}) = \int_{R(y_1)} |J(y_1,y_2)| f_{\mathbf{Y}}(y_1,y_2|E_{Yi}) dy_2,$$
$$= \frac{1}{|w_{1i}|}\int_{R(y_1)} f_{\mathbf{H}}\left(\frac{y_1 - w_{2i}y_2}{w_{1i}}, y_2\middle|E_{Hi}\right) dy_2,$$

where the integral is over the region $R(y_1) = \{y_2 : f_{\mathbf{Y}}(y_1,y_2|E_{Yi}) > 0\}$. It can be verified that the PDF of $\mathbf{Y_1}$ is symmetric about 0. So, the PDF of the random variable $\mathbf{D} = |\mathbf{Y_1}|$ can be computed as $f_{\mathbf{D}}(d|E_{Yi}) = 2f_{\mathbf{Y_1}}(d|E_{Yi}), \ \ d \geq 0$. Applying the limit $d \to 0$, we have

$$\lim_{d\to 0} f_{\mathbf{D}}(d|E_{Yi}) = \lim_{d\to 0} 2f_{\mathbf{Y_1}}(d|E_{Yi}),$$
$$= \lim_{d\to 0}\frac{2}{|w_{1i}|}\int_{R(d)} f_{\mathbf{H}}\left(\frac{d - w_{2i}y_2}{w_{1i}}, y_2\middle|E_{Hi}\right) dy_2,$$
$$= \frac{2}{|w_{1i}|}\int_{-\infty}^{\infty}\lim_{d\to 0} f_{\mathbf{H}}\left(\frac{d - w_{2i}y_2}{w_{1i}}, y_2\middle|E_{Hi}\right) dy_2,$$
$$= \frac{2}{2\pi\sigma_h^2|w_{1i}|P_{Hi}}\int_{-\infty}^{\infty}\exp\left(-\frac{y_2^2}{2\sigma_h^2}\left(1+\frac{w_{2i}^2}{w_{1i}^2}\right)\right) dy_2,$$
$$= \frac{1}{\sigma_h P_{Hi}}\sqrt{\frac{2}{\pi}}\frac{1}{\sqrt{w_{1i}^2 + w_{2i}^2}}.$$

In the third step, the limit $d \to 0$ is moved inside the integration. This can be justified based on Bounded convergence theorem. According to this, if a sequence of functions $\{g_n(x)\}$ converges to the function $g(x)$, where $|g_n(x)| \leq K$ for all n and $g(x)$ is integrable, then $\int g_n(x)$ converges to $\int g(x)$. In our case, $f_{\mathbf{H}} \leq \frac{1}{2\pi\sigma_h^2}$ and $\lim_{d\to 0} f_{\mathbf{H}}(\ )$ is integrable. Also, in the limit $d \to 0$, the region of integration $R(d) = R(0) = \{y_2 : f_{\mathbf{Y}}(0,y_2|E_{Yi}) > 0\} = (-\infty,\infty)$. This can be justified as follows: At $\frac{h_2}{h_1} = \alpha_i, i \in$ NRI, we have $d(f_i,h_1,h_2) = w_{1i}h_1 + w_{2i}h_2 = 0$. So, as per the transformation in (26), (27), the region $S_{Hi} = \{(h_1,h_2) : h_2 = \alpha_i h_1\}$ maps to the region $S_{Yi} = \{y_1,y_2 : y_1 = 0, y_2 \in (-\infty,\infty)\}$. From (28), we have $f_{\mathbf{H}}(h_1,h_2|E_{Hi}) > 0 \ \forall \ (h_1,h_2) \in S_{Hi}$. So, $f_{\mathbf{Y}}(y_1,y_2|E_{Yi}) > 0 \ \forall \ (y_1,y_2) \in S_{Yi}$. Hence, $R(0) = (-\infty,\infty)$. Since the events E_{Yi} and E_{Hi} are equivalent, we have (6).

B. PDF of minimum cluster distance in the region $B_H^\epsilon(h_2 = 0)$ for M-PAM

Let $\mathbf{H}$ be the random vector corresponding to $H = [h_1\, h_2]$. The PDF of $\mathbf{H}$ conditioned on the event E_{h_2} is computed as

$$f_{\mathbf{H}}(h_1,h_2|E_{h_2}) = \frac{1}{2\pi\sigma_h^2 P_{h_2}}\exp\left(-\frac{h_1^2+h_2^2}{2\sigma_h^2}\right), \quad (h_1,h_2) \in B_H^\epsilon(h_2 = 0),$$

where $P_{h_2} = \Pr(E_{h_2})$. The PDF of the random variable $\mathbf{H_2}$ corresponding to h_2 can be computed by marginalizing the PDF of $\mathbf{H}$. The PDF of $\mathbf{H_2}$ is symmetric about 0. So, the PDF of the random variable $\mathbf{D} = 2|\mathbf{H_2}|$ is computed as $f_{\mathbf{D}}(d|E_{h_2}) = f_{\mathbf{H_2}}\left(\frac{d}{2}\middle|E_{h_2}\right), \ d \geq 0$. Applying the limit $d \to 0$, we can show that,

$$\lim_{d\to 0} f_{\mathbf{D}}(d|E_{h_2}) = \frac{1}{\sigma_h\sqrt{2\pi}P_{h_2}}.$$

C. PDF of left and right minimum cluster distance in the region $B_H^\epsilon(h_2 = 0)$ for M-PAM

In this section, we compute $\lim_{d\to 0} f_{\mathbf{D_{L(1,p)}}}(d|E_{h_2})$. We consider the cases $p = 1$ and $p \neq 1$ separately. First, let us consider the case $p = 1$. Let $(h_1,h_2) \in B_H^\epsilon(h_2 = 0)$. Consider the symbol pair $(2l - M - 1, v_1) \in \Lambda_l$. This corresponds to the point $r_1 = (2l - M - 1)h_1 + v_1 h_2 \in T_l$, which is the left most point in $\mathcal{M}_B$ among the points in T_l. So, the left minimum cluster distance in $\mathcal{M}_B$ with reference to $(2l - M - 1, v_1)$ is $d_{L(l,1)} = |r_1 - r_2|$, for some $r_2 \in T_q, q \neq l$. It can be proved that $|r_1 - r_2| > 0 \ \forall \ (h_1,h_2) \in B_H^\epsilon(h_2 = 0)$. So, we have

$$\lim_{d\to 0} f_{\mathbf{D_{L(1,p)}}}(d|E_{h_2}) = 0, \quad p = 1.$$

Next, we consider the case $p \neq 1$. Consider the point $r_1 = (2l - M - 1)h_1 + v_p h_2 \in T_l$. The point $r_2 = (2l - M - 1)h_1 + v_{p-1}h_2 \in T_l$ is to the left of r_1 as per the ordering in T_l. We have $|r_1 - r_2| = 2|h_2|$ (refer section III-D1), which is also the minimum cluster distance in $\mathcal{M}_B$ in the region $B_H^\epsilon(h_2 = 0)$. So, r_2 is adjacent, and to the left of r_2, in $\mathcal{M}_B$. Also, r_1 and r_2 correspond to transmit pairs from different clusters. So, the left minimum cluster distance in $\mathcal{M}_B$ with reference to $(2l - M - 1, v_p)$ is $2|h_2|$. We have

$$\lim_{d\to 0} f_{\mathbf{D_{L(1,p)}}}(d|E_{h_2}) = \frac{1}{\sigma_h P_{h_2}\sqrt{2\pi}}, \quad p = 2, 3, \cdots M, \quad (29)$$

which follows from results in section VI-B. Similarly, we can derive

$$\lim_{d\to 0} f_{\mathbf{D_{R(1,p)}}}(d|E_{h_2}) = \begin{cases} 0, & p = M, \\ \frac{1}{\sigma_h P_{h_1}\sqrt{2\pi}}, & p = 1, 2, \cdots M-1. \end{cases}$$

References

[1] S. Zhang, S. C. Liew, and P. P. Lam, "Hot topic: Physical-layer network coding," in *Proceedings of the 12th Annual International Conference on Mobile Computing and Networking*, ser. MobiCom '06, 2006, pp. 358–365.

[2] P. Popovski and H. Yomo, "The anti-packets can increase the achievable throughput of a wireless multi-hop network," in *Communications, 2006. ICC '06. IEEE International Conference on*, vol. 9, 2006, pp. 3885–3890.

[3] B. Nazer and M. Gastpar, "Computing over multiple-access channels with connections to wireless network coding," in *Information Theory, 2006 IEEE International Symposium on*, 2006, pp. 1354–1358.

[4] P. Popovski and T. Koike-Akino, "Coded bidirectional relaying in wireless networks," in *New Directions in Wireless Communications Research*, V. Tarokh, Ed. Springer, Sep. 2009, pp. 291–316.

[5] B. Nazer and M. Gastpar, "Reliable physical layer network coding," *Proceedings of the IEEE*, vol. 99, no. 3, pp. 438–460, March 2011.

[6] M. Wilson, K. Narayanan, H. Pfister, and A. Sprintson, "Joint physical layer coding and network coding for bidirectional relaying," *Information Theory, IEEE Transactions on*, vol. 56, no. 11, pp. 5641–5654, Nov. 2010.

[7] W. Nam, S.-Y. Chung, and Y. Lee, "Capacity of the Gaussian two-way relay channel to within bit," *Information Theory, IEEE Transactions on*, vol. 56, no. 11, pp. 5488–5494, nov. 2010.

[8] S. Zhang and S.-C. Liew, "Channel coding and decoding in a relay system operated with physical-layer network coding," *Selected Areas in Communications, IEEE Journal on*, vol. 27, no. 5, pp. 788–796, June 2009.

[9] Z. Faraji-Dana and P. Mitran, "On non-binary constellations for channel-coded physical-layer network coding," *Wireless Communications, IEEE Transactions on*, vol. 12, no. 1, pp. 312–319, 2013.

[10] B. Hern and K. Narayanan, "Multilevel coding schemes for compute-and-forward with flexible decoding," *Information Theory, IEEE Transactions on*, vol. 59, no. 11, pp. 7613–7631, Nov 2013.

[11] T. Koike-Akino, P. Popovski, and V. Tarokh, "Optimized constellations for two-way wireless relaying with physical network coding," *Selected Areas in Communications, IEEE Journal on*, vol. 27, no. 5, pp. 773–787, 2009.

[12] V. Muralidharan, V. Namboodiri, and B. Rajan, "Wireless network-coded bidirectional relaying using latin squares for M-PSK modulation," *Information Theory, IEEE Transactions on*, vol. 59, no. 10, pp. 6683–6711, 2013.

[13] V. Namboodiri, K. Venugopal, and B. Rajan, "Physical layer network coding for two-way relaying with QAM," *Wireless Communications, IEEE Transactions on*, vol. 12, no. 10, pp. 5074–5086, 2013.

[14] K. Ravindran, A. Thangaraj, and S. Bhashyam, "Ldpc codes for network-coded bidirectional relaying with higher order modulation," *Communications, IEEE Transactions on*, vol. 63, no. 6, pp. 1975–1987, June 2015.

[15] O. Dabeer and E. Masry, "Asymptotic behavior of the pairwise error probability with applications to transmit beamforming and rake receivers," *Wireless Communications, IEEE Transactions on*, vol. 4, no. 2, pp. 444–452, March 2005.

[16] T. Huang, J. Yuan, and J. Li, "Analysis of compute-and-forward with qpsk in two-way relay fading channels," in *Communications Theory Workshop (AusCTW), 2013 Australian*, Jan 2013, pp. 75–80.

[17] T. Yang and I. Collings, "Asymptotically optimal error-rate performance of linear physical-layer network coding in rayleigh fading two-way relay channels," *Communications Letters, IEEE*, vol. 16, no. 7, pp. 1068–1071, July 2012.

[18] M. Ju and I.-M. Kim, "Error performance analysis of bpsk modulation in physical-layer network-coded bidirectional relay networks," *Communications, IEEE Transactions on*, vol. 58, no. 10, pp. 2770–2775, October 2010.

[19] E. Peh, Y.-C. Liang, and Y. L. Guan, "Power control for physical-layer network coding in fading environments," in *Personal, Indoor and Mobile Radio Communications, 2008. PIMRC 2008. IEEE 19th International Symposium on*, Sept 2008, pp. 1–5.

[20] S. H. Kim, B. C. Jung, and D. K. Sung, "Transmit power optimization for two-way relay channels with physical-layer network coding," *Communications Letters, IEEE*, vol. 19, no. 2, pp. 151–154, Feb 2015.

[21] B. Nazer and M. Gastpar, "Compute-and-forward: Harnessing interference through structured codes," *IEEE Transactions on Information Theory*, vol. 57, no. 10, pp. 6463–6486, Oct 2011.

[22] Z. Chen, B. Xia, Z. Hu, and H. Liu, "Design and analysis of multi-level physical-layer network coding for gaussian two-way relay channels," *IEEE Transactions on Communications*, vol. 62, no. 6, pp. 1803–1817, June 2014.

[23] Y. C. Huang, K. R. Narayanan, and P. C. Wang, "Adaptive compute-and-forward with lattice codes over algebraic integers," in *2015 IEEE International Symposium on Information Theory (ISIT)*, June 2015, pp. 566–570.

[24] T. Yang and I. B. Collings, "On the optimal design and performance of linear physical-layer network coding for fading two-way relay channels," *IEEE Transactions on Wireless Communications*, vol. 13, no. 2, pp. 956–967, February 2014.

[25] D. Fang, A. Burr, and J. Yuan, "Linear physical-layer network coding over hybrid finite ring for Rayleigh fading two-way relay channels," *Communications, IEEE Transactions on*, vol. 62, no. 9, pp. 3249–3261, Sept 2014.